



Physico-chemical characterisation and photocatalytic activity of nanosized $\text{SO}_4^{2-}/\text{TiO}_2$ towards degradation of 4-nitrophenol

Santosh Kumar Samantaray, Priyabrat Mohapatra, Kulamani Parida*

EM & IC Department, Regional Research Laboratory (CSIR), Bhubaneswar 751013, Orissa, India

Received 10 October 2002; accepted 4 December 2002

Abstract

Unmodified and sulphate-modified TiO_2 samples of different crystal forms and crystal sizes were prepared at different pH, varying the source and concentration of sulphate ion and by activating at different temperatures. The samples were characterised by XRD, FT-IR, TEM and nitrogen adsorption–desorption methods. The TEM and XRD patterns revealed that TiO_2 sample prepared at lower pH (pH 3) exhibit smaller crystallite size than that of higher pH (pH 9). Sulphate ion impregnation also decreases the crystallite size and stabilises the anatase phase of TiO_2 at higher activation temperatures. FT-IR results show that sulphate species strongly bound bidentately on TiO_2 surface. Surface area is more in case of sample prepared at lower pH than that of higher pH and also found to increase with the increase in sulphate loading up to 7.5 wt.% and thereafter decreases drastically. The photocatalytic activities of the catalysts were compared by performing degradation of 4-nitrophenol as a probe reaction. Photocatalytic degradation of 4-nitrophenol depends on surface area, the crystal form and particle size of TiO_2 . Samples containing mixture of anatase and rutile phases exhibit highest activity for degradation of 4-nitrophenol than that of other samples.

© 2002 Elsevier Science B.V. All rights reserved.

Keywords: Sulphated TiO_2 ; Crystal forms and size; Activation temperature; Photocatalytic degradation; 4-Nitrophenol

1. Introduction

Nitrophenols are some of the most refractory pollutants, which can be present in industrial wastewater. In particular, 4-nitrophenol and its derivatives result from the production processes of pesticides, herbicides [1] and synthetic dyes [2]. These pollutants have high toxicity and carcinogenic character. They have caused considerably damage to the ecosystem and human health. Traditional wastewater treatment includes activated carbon adsorption, chemical

oxidation, biological digestion, etc. However, there are some limitations in each technique. The feasibility of wastewaters containing 4-nitrophenol being subjected to an ozonisation process was investigated by Beltran et al. [3], whereas Pintar and Levec [4] studied catalytic oxidation in a temperature range of 423–463 K. The photocatalytic abatement of 4-nitrophenol in TiO_2 aqueous slurries have been investigated [1,5–12]. The possibility of sensitised photocatalytic degradation at pH 8.5 was demonstrated in [1] and the effects of catalyst load and of oxygen and organic concentration was mainly focused in [5], disregarding pH. Whereas earlier [9,10] and recent [6–8] literature reported the reaction mechanism and the kinetic models.

* Corresponding author. Tel.: +91-674-581636-305;
fax: +91-674-581637.
E-mail address: kmparida@yahoo.com (K. Parida).

The pore structure, pore size, particle size and activation temperature of TiO₂ affects the photocatalytic activity of organic pollutants in wastewater [13–17]. The surface and textural properties of TiO₂ depend greatly on the method of preparation and activation temperature. Our earlier studies [18–20] revealed that the method of preparation, source and concentration of anions affected the surface, textural as well as catalytic activities of TiO₂ towards acid-catalysed reactions. A few reports are available on SO₄²⁻/TiO₂ for photocatalytic degradation of CH₃Br [21], NO₂⁻ [22] and textile wastewater [23].

In order to understand the effect of anions on the crystallite size of TiO₂, we have prepared hydrated TiO₂ at different pH and modified this by varying the source and concentration of anions using different techniques. The unmodified and modified TiO₂ samples are activated at different temperatures and their activities toward photochemical degradation of 4-nitrophenol are studied.

2. Experimental

2.1. Materials and methods

Hydrated titania was prepared at pH 3, 5, 7 and 9 by adding aqueous ammonia to the stirred aqueous solution of titanium tetrachloride. Obtained gel was filtered and washed repeatedly to remove Cl⁻ (negative AgNO₃ test), dried at 383 K for 10 h, powdered to 45–75 μm mesh size and kept for anion impregnation.

2.2. Modified catalysts

One series of sulphated titania samples with varying the weight percentage of SO₄²⁻ were prepared using (NH₄)₂SO₄ as the source of sulphate ions by solid–solid kneading method and the other series of samples were prepared by aqueous wetness impregnation method using dilute H₂SO₄ (strength = 1.0 M). The suspended mass was evaporated to dryness on a hot plate while stirring. The samples were then dried in an air oven at 383 K and subsequent activation (by calcination) at 573, 673, 773, 873, 973 and 1073 K at the heating rate of 283 K/min in a muffle furnace for 3 h.

3. Characterisation

3.1. Powder X-ray diffraction

The XRD patterns of pure and modified TiO₂ samples were recorded on a Philips X-ray diffractometer having a PW 1830 generator with copper tube, a PW 1820 goniometer fitted with a post-diffracted graphite monochromator and a scintillation detector attached to a PW 1710 diffraction control in the range of 2θ = 6–80° at a scanning speed of 2°/min. The instrument was operated at 40 kV and 20 mA. The average crystallite size (*L*) was determined by XRD line broadening technique using the Debye–Scherrer equation:

$$L = \frac{0.94\lambda}{b \cos \theta} \quad (1)$$

where λ is the wavelength of the X-ray used and *b* the relative peak broadening, calculated as $b^2 = b_{\text{exp}}^2 - b_{\text{ref}}^2$, where *b*_{exp} and *b*_{ref} are half-widths at maxima observed on a given sample and on a reference material which is ideally crystalline, respectively.

3.2. FT-IR study

The FT-IR spectra of pure and modified TiO₂ samples were recorded with a Perkin-Elmer (model: Paragon 500) FT-IR spectrometer in the range of 4000–400 cm⁻¹ on palletised with KBr phase (spectrophotometric grade). All the samples were degassed at 383 K in vacuum (1 × 10⁻⁴ Torr) before analysis. However, after evacuation in vacuum at 383 K, the samples only retained the ligated water.

3.3. Transmission electron microscope

The morphologies of the samples were examined using a Hitachi H-600 transmission electron microscope (TEM).

3.4. Textural properties

Surface area (BET), average pore radius and pore size distributions were determined by the N₂ adsorption–desorption method at liquid nitrogen temperature using quantasorb (Quantachrome, USA). Prior to adsorption–desorption measurements, the samples were degassed at 393 K and 10⁻⁴ Torr for 5 h.

3.5. Catalytic activity

The photocatalytic degradation of 4-nitrophenol was performed taking 0.05 g/l of substrate (4-nitrophenol in water, CDH) and 0.2 g/l of catalyst. The pH of the dispersion was adjusted by addition of sulphuric acid (BDH). The solutions were exposed to sunlight in closed Pyrex flasks at room temperature (no extra cooling) with constant stirring. All the irradiation was performed during the second half of March 2002 (sunny days), from 11:00 to 14:00 h and was repeated three times. The corresponding dark controls were carried out simultaneously, for comparison. After irradiation taking at different times, the suspension was filtered and 4-nitrophenol was analysed quantitatively by measuring the absorption at 315 nm using Cary-1E (Varian) spectrophotometer. The detail method for measurement was available in [5].

4. Results and discussion

Transmission electron microscope images of the unmodified and sulphate-modified TiO₂ samples are shown in Fig. 1a–d. It is observed that TiO₂ sample prepared at pH 3 (Fig. 1a) possesses uniform, finely distributed TiO₂ particles of size ~12 nm. However, the particles of the samples prepared at pH 9 are clumped to each other forming agglomerates and lies around ~20 nm (Fig. 1b). The particle size sharply decreases to 2–3 nm (Fig. 1c and d) in the sulphate-modified sample.

The powder X-ray diffraction patterns of TiO₂ prepared at different pH and activated at 773 K are shown

in Fig. 2. It can be seen that samples prepared at pH 3 possess mixture of anatase and rutile phases whereas at pH 5, 7 and 9 possess only anatase phase. From the XRD pattern (Fig. 3), it has been found that unmodified TiO₂ sample prepared at pH 3 and activated up to 673 K possess only anatase phase. With increasing the activation temperature up to 773 K both anatase and rutile phases are found (Fig. 2a). Whereas sample activated at 873 K possess only rutile phase. However, TiO₂ samples prepared at pH 3, modified with sulphate ion and activated up to 873 K possesses only anatase phase (Fig. 4). With increasing the activation temperature up to 973 K both anatase and rutile phases are found. But in the sample activated at 1073 K only rutile phase is observed. So, it may be concluded that sulphate ion stabilises the anatase phase of TiO₂ up to 973 K activation temperature. It is also observed that (Fig. 5) sulphate-modified TiO₂ samples activated at 773 K possess anatase phase, irrespective of the source and percentage of sulphate loading. There is no indication of formation of titanium sulphate in any one of the samples; even in 10 wt.% SO₄²⁻ impregnation. This type of observation was also reported earlier [18–20] in TiO₂ samples prepared at pH 7 and modified with phosphate and sulphate ions.

To develop a better understanding of formation and crystallisation in the presence of sulphate ion, the average crystallite size (*L*) perpendicular to the (210) plane was calculated from the XRD patterns of pure and sulphated titania. It is seen (Table 1) that the crystallite size of titania sample prepared at pH 3 is lesser than the sample prepared at pH 9. It gradually increases with increasing the pH of the solution, which suppresses the growth of the particle, may be due

Table 1
Average crystallite size of unmodified and modified TiO₂ samples activated at different temperatures

Sample code	Crystallite size (nm)	Sample code	Crystallite size (nm)
TiO ₂ , pH 3, 773 K	13.2	TiO ₂ , pH 3, 383 K	8.7
TiO ₂ , pH 5, 773 K	14.5	TiO ₂ , pH 3, 573 K	9.5
TiO ₂ , pH 7, 773 K	16.1	TiO ₂ , pH 3, 673 K	14.8
TiO ₂ , pH 9, 773 K	17.2	TiO ₂ , pH 3, 873 K	0.0
2.5SO ₄ ²⁻ /TiO ₂ , pH 3, 773 K	5.2	2.5SO ₄ ²⁻ /TiO ₂ (H), pH 3, 573 K	3.1
5.0SO ₄ ²⁻ /TiO ₂ , pH 3, 773 K	4.7	2.5SO ₄ ²⁻ /TiO ₂ (H), pH 3, 673 K	3.4
7.5SO ₄ ²⁻ /TiO ₂ , pH 3, 773 K	4.3	2.5SO ₄ ²⁻ /TiO ₂ (H), pH 3, 773 K	3.5
7.5SO ₄ ²⁻ /TiO ₂ (H), pH 3, 773 K	3.5	2.5SO ₄ ²⁻ /TiO ₂ (H), pH 3, 873 K	3.8
10SO ₄ ²⁻ /TiO ₂ , pH 3, 773 K	4.2	2.5SO ₄ ²⁻ /TiO ₂ (H), pH 3, 973 K	2.7

Note: (H) indicates the sample prepared from H₂SO₄.

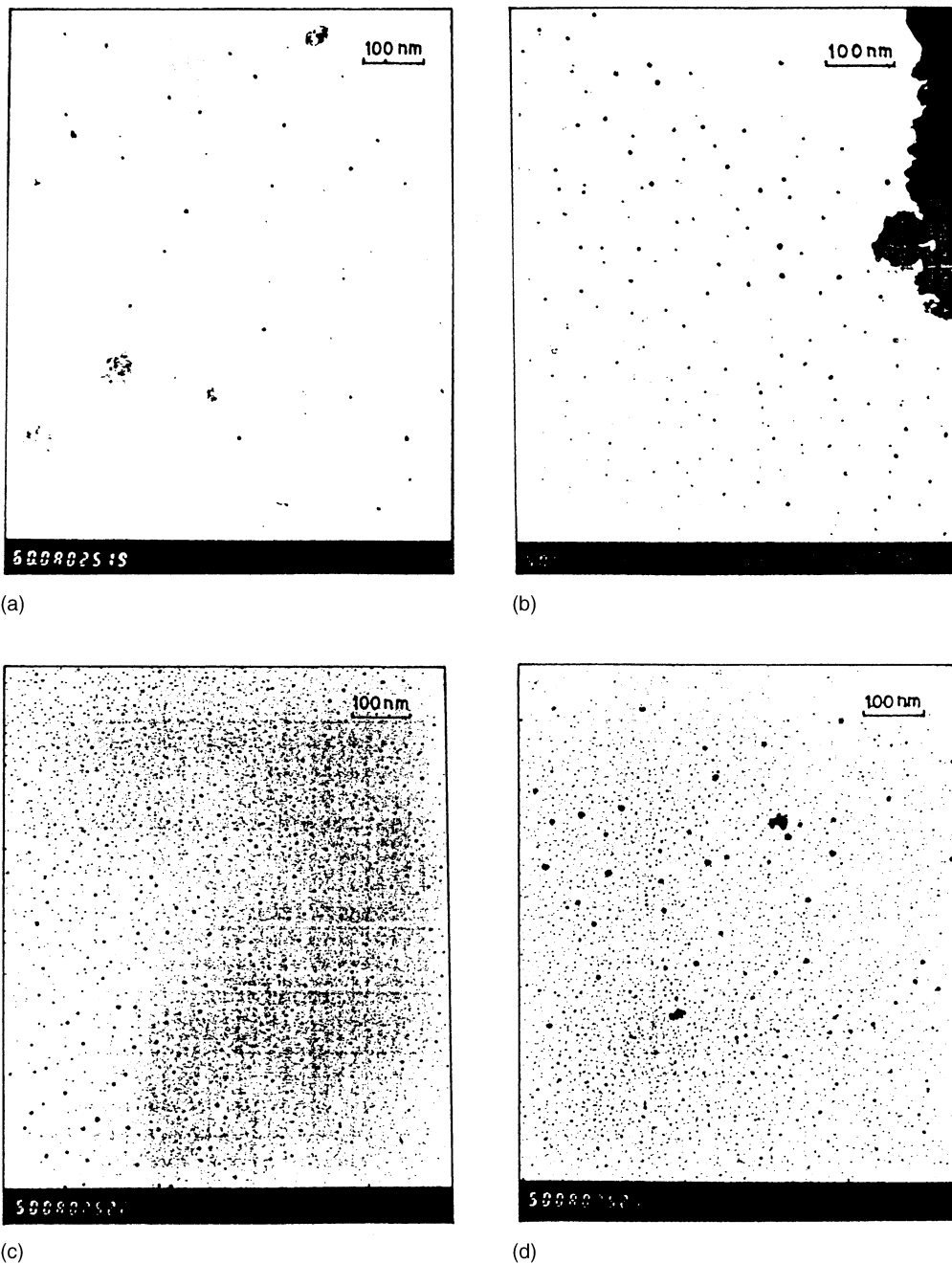


Fig. 1. TEM photographs of: (a) TiO_2 , pH 3, 773 K; (b) TiO_2 , pH 9, 773 K; (c) $2.5\text{SO}_4^{2-}/\text{TiO}_2$, pH 3, 773 K; (d) $2.5\text{SO}_4^{2-}/\text{TiO}_2$, pH 3, 973 K.

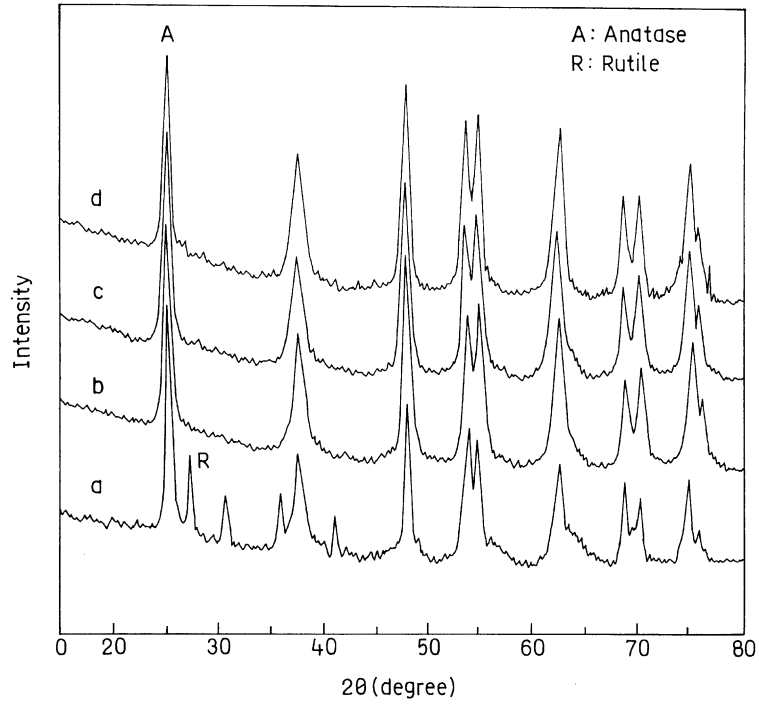


Fig. 2. Powder XRD patterns of TiO₂ samples prepared at: (a) pH 3; (b) pH 5; (c) pH 7; (d) pH 9, activated at 773 K.

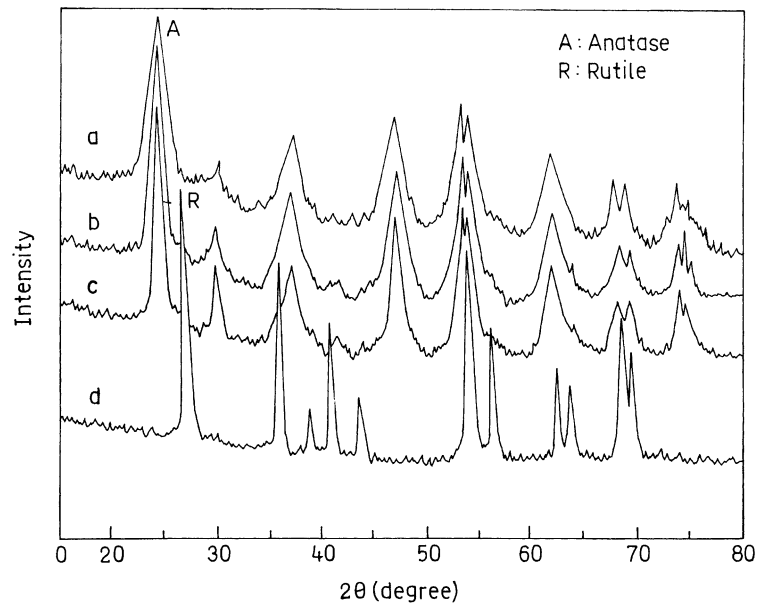


Fig. 3. Powder XRD patterns of TiO₂ sample prepared at pH 3, activated at: (a) 383 K; (b) 573 K; (c) 673 K; (d) 873 K.

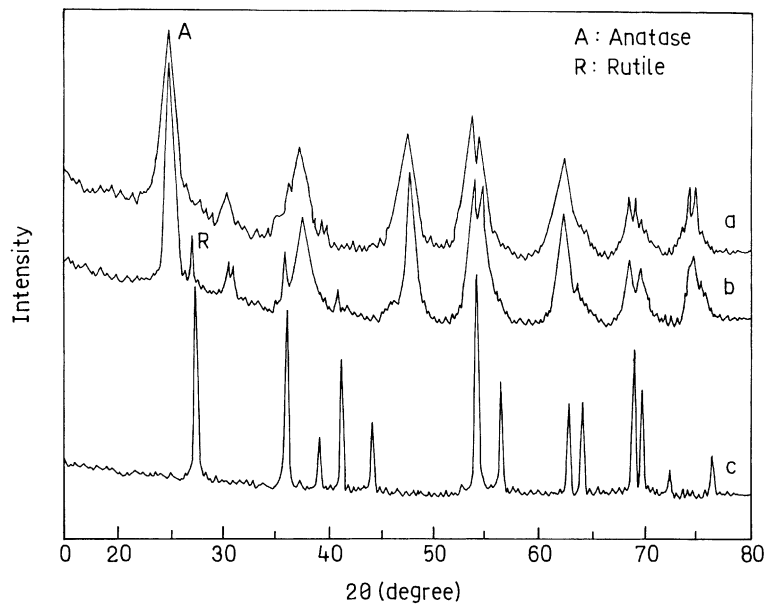


Fig. 4. Powder XRD patterns of $2.5\text{SO}_4^{2-}/\text{TiO}_2$ sample prepared at pH 3, activated at: (a) 873 K; (b) 973 K; (c) 1073 K.

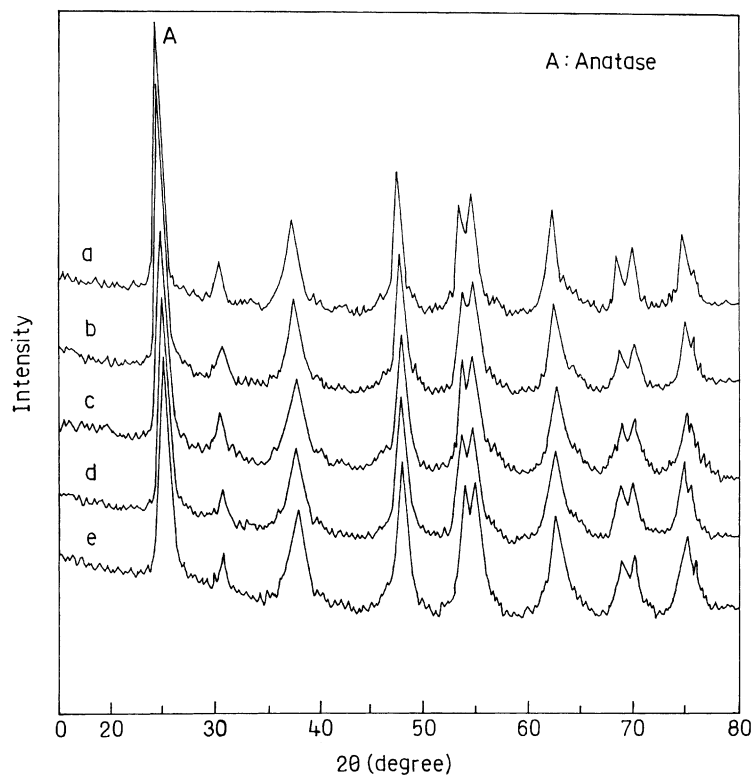


Fig. 5. Powder XRD patterns of: (a) $2.5\text{SO}_4^{2-}/\text{TiO}_2(\text{H})$; (b) $5.0\text{SO}_4^{2-}/\text{TiO}_2(\text{H})$; (c) $7.5\text{SO}_4^{2-}/\text{TiO}_2(\text{H})$; (d) $7.5\text{SO}_4^{2-}/\text{TiO}_2$; (e) $10.0\text{SO}_4^{2-}/\text{TiO}_2(\text{H})$, activated at 773 K.

to rapid hydrolysis (spontaneous nucleation) [24,25]. It is observed that the crystallite size of titania decreases with 2.5 wt.% SO_4^{2-} loading and thereafter it remained almost unchanged. However, the effect is more pronounced with sulphuric acid as the source of sulphate compared to $(\text{NH}_4)_2\text{SO}_4$. This indicates that the crystallinity is more or less dependent on the presence of sulphate ion, but not on the source and percentage of sulphate loading. In addition to stabilising anatase TiO_2 crystallites, sulphate surface species inhibit TiO_2 crystallite sintering, leading to smaller crystallites than in pure TiO_2 . The crystallite size decreases in the presence of sulphate ions as SO_4^{2-} species could possibly interact with TiO_2 network, and thus hinder the growth of the particle. Even a very small amount of SO_4^{2-} species is responsible for this effect. Therefore, the change in sulphate concentration did not change crystallite size further. Therefore, it is assumed that small amount of sulphate species

is responsible for the lowering of crystallite size. It is also observed that crystallite size of unmodified TiO_2 increases with increase in activation temperature from 383 to 673 K and thereafter it decreases. The increase in crystallite size may be due to desorption of surface hydroxyl group from the TiO_2 network and the decrease is perhaps due to the formation of rutile phase. However, crystallite size remains almost constant up to 873 K and thereafter decreases in case of sulphate-modified TiO_2 . This suggests that sulphate species strongly interacting with TiO_2 crystallites inhibits sintering even at higher activation temperatures. This type of effect is also observed in PO_4^{3-} -modified $\text{FeO}(\text{OH})$ [26], WO_3 -modified ZrO_2 [27] and TiO_2 [28].

FT-IR spectra of sulphated metal oxides generally show a strong absorption band at 1381 cm^{-1} , and broad bands at $1250\text{--}1100\text{ cm}^{-1}$ (Fig. 6). The 1381 cm^{-1} peak is the stretching frequency of $\text{S}=\text{O}$,

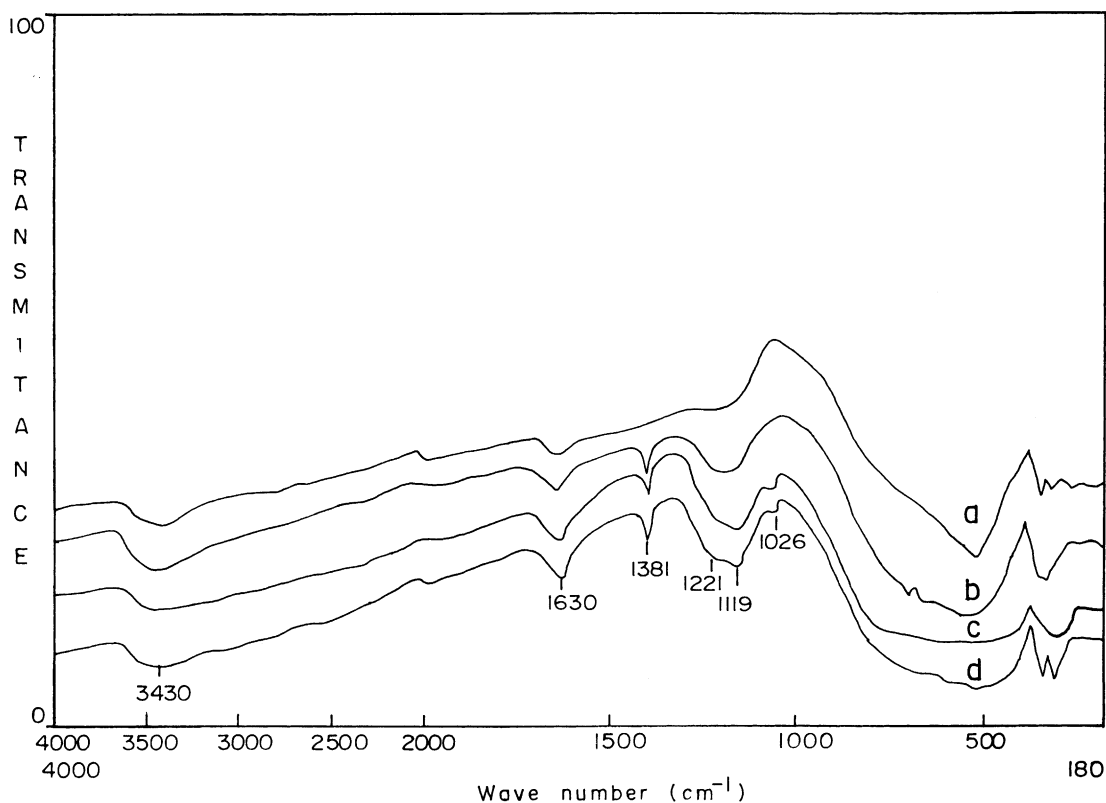


Fig. 6. FT-IR spectra of: (a) TiO_2 ; (b) $2.5\text{SO}_4^{2-}/\text{TiO}_2$; (c) $7.5\text{SO}_4^{2-}/\text{TiO}_2$; (d) $7.5\text{SO}_4^{2-}/\text{TiO}_2(\text{H})$, activated at 773 K.

and the 1250–1100 cm^{-1} peaks are the characteristic frequencies of SO_4^{2-} . The broad bands at 1250–1100 cm^{-1} resulted from the lowering of the symmetry in the free SO_4^{2-} (Td point group). When SO_4^{2-} is bound to the titania surface, the symmetry can be lowered to either C_{3V} or C_{2V} [29]. Here, the band that split into three peaks (1221, 1119 and 1026 cm^{-1}) was assigned to the bidentately bound sulphate group (C_{2V} point group). The bands at 1630 and 3430 cm^{-1} correspond to the bending and stretching of OH group of water molecules occluded in the sample, respectively.

It is observed (Table 2) that with an increase in sulphate loading increase the surface area up to 7.5 wt.% (from 64 to 102 m^2/g). Further increase in sulphate loading to 10 wt.% resulted in a decrease in surface area (95 m^2/g). The trend remains the same irrespective of the source of sulphate ion. Similar trend is also maintained in case of the pore volume. Therefore, the presence of low amount of sulphate ion (≤ 7.5 wt.%) may be responsible in the formation of porous network. It has been shown [30,31] that, in sulphated metal oxides, some of the hydroxyl bridges originally present in dried uncalcined and unsulphated titania replaced the sulphate ions. On calcination, the formation of oxybonds takes place, and results in changes in the Ti–O–Ti bond strength due to attachment of the sulphate bridges. Thus, the changes in the Ti–O–Ti bond strength may be responsible for the formation of porous network. Consequently, the increase in surface area with an increase in sulphate loading up to 7.5 wt.% appears to be due to the stabilising effect of the sulphate ions. However, the plugging of more pores may have occurred with higher sulphate loading resulting in a reduction of total pore volume to some extent and also decrease in surface area [30]. With increase in activation temperature, the surface area decreases gradually. This might be due to the inter-particle agglomeration or due to collapse of very fine/narrow pores. It is also observed that the surface area gradually decreases with increase in pH of the hydrolysis. Sample prepared at pH 3 has higher surface area compared to the sample prepared at pH 9. This type of observation is also reported earlier [32].

From the preliminary study, no degradation of nitrophenol was observed in the absence of light and/or of catalyst. Fig. 7 represents the effect of pH (adjusted by H_2SO_4) of the solution on the photocatalytic

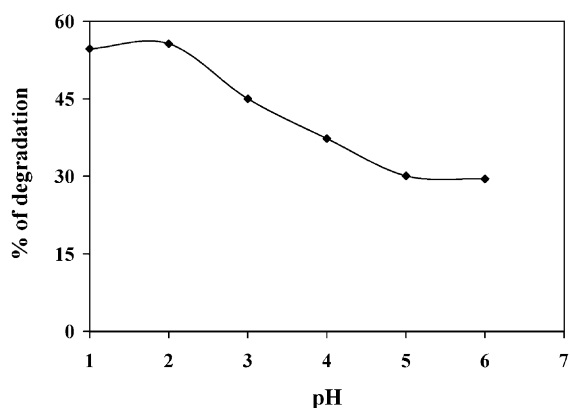


Fig. 7. Effect of solution pH (by H_2SO_4) on the percentage of degradation.

degradation of 4-nitrophenol. It is found that with increasing the pH of the solution up to 2, the percentage of 4-nitrophenol degradation remains almost constant. However, after that it decreases gradually with increasing the pH of the solution. Since no nitrobenzene was detected during the photolysis of 4-nitrophenol at pH 2, it can be concluded that the reductive pathway is favoured in acidic media. It is known that nitroaromatic compounds such as 4-nitrophenol are reduced in acidic media more easily than in alkaline solutions [33].

Fig. 8 represents the effect of TiO_2 samples prepared at different pH on the photocatalytic degradation

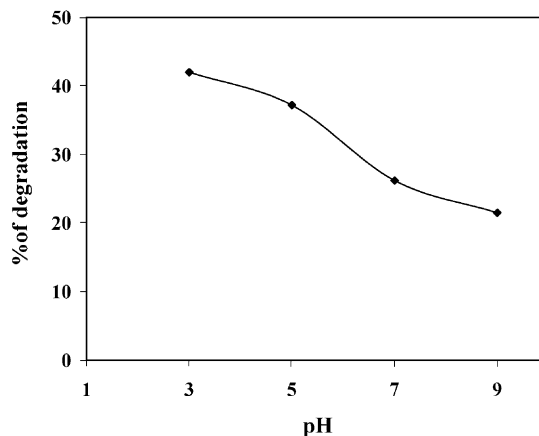


Fig. 8. Effect of preparation condition (pH) of catalyst on the percentage of degradation.

Table 2

Specific surface area (BET) of unmodified and modified TiO₂ samples activated at different temperatures

Sample code	S _{BET} (m ² /g)	Sample code	S _{BET} (m ² /g)
TiO ₂ , pH 3, 773 K	64	TiO ₂ , pH 3, 383 K	174
TiO ₂ , pH 5, 773 K	60	TiO ₂ , pH 3, 573 K	150
TiO ₂ , pH 7, 773 K	57	TiO ₂ , pH 3, 673 K	74
TiO ₂ , pH 9, 773 K	46	TiO ₂ , pH 3, 873 K	22
2.5SO ₄ ²⁻ /TiO ₂ , pH 3, 773 K	74	2.5SO ₄ ²⁻ /TiO ₂ (H), pH 3, 383 K	210
5.0SO ₄ ²⁻ /TiO ₂ , pH 3, 773 K	83	2.5SO ₄ ²⁻ /TiO ₂ (H), pH 3, 573 K	180
7.5SO ₄ ²⁻ /TiO ₂ , pH 3, 773 K	102	2.5SO ₄ ²⁻ /TiO ₂ (H), pH 3, 673 K	139
7.5SO ₄ ²⁻ /TiO ₂ (H), pH 3, 773 K	114	2.5SO ₄ ²⁻ /TiO ₂ (H), pH 3, 873 K	29
10SO ₄ ²⁻ /TiO ₂ , pH 3, 773 K	95	2.5SO ₄ ²⁻ /TiO ₂ (H), pH 3, 973 K	2

Note: (H) indicates the sample prepared from H₂SO₄.

of 4-nitrophenol. It is observed that with increasing the pH of the precipitation the percentage of degradation gradually decreases. This may be due to higher surface area, lower porosity and crystallite size, and more number of hydroxyl groups present on the TiO₂ sample prepared at lower pH than that of higher pH. As reported earlier [5,34,35], the surface hydroxyl groups bound to titanium atoms constitute the adsorption active sites. The large amount of hydroxyl groups on the surface of titania might have trap the holes in the valence band and enhance the chemisorption of dissolved O₂ or •OH radical in the conduction band. The pH variation on the preparation procedure affects the adsorption capacity of the gel because it affects the surface area as well as crystallite size and hence the number of surface hydroxyl groups. As reported earlier [36], the mixture of anatase and rutile phases of TiO₂ is more active than either anatase or rutile crystallites at the same activation temperature. Here, it is also observed from the XRD pattern of TiO₂ sample prepared at pH 3 and activated at 773 K shows both anatase and rutile phases. Whereas other samples prepared at pH 5, 7 and 9 exhibits only anatase phase at similar activation temperature. The presence of mixture of anatase and rutile phases in sample prepared at pH 3 increases the surface area may be due to wider range pore size distribution which is responsible for the increase in catalytic activity by effective adsorption of 4-nitrophenol [36–38].

Fig. 9 represents the effect of wt.% of sulphate in TiO₂ on the photocatalytic degradation of 4-nitrophenol. It is observed that with the addition of 2.5 wt.% of sulphate on TiO₂ the percentage of

degradation increases. However, further addition of higher sulphate content does not affect more to the percentage of degradation. This may be due to the addition of small amount of sulphate decreases the crystallite size of titania, which facilitates higher percentage of degradation. The reason may be due to the so-called particle size quantisation effect. A blue shift in absorption spectra is usually observed when the size of semiconductor particles becomes small [39]. However, increasing the wt.% of sulphate on TiO₂ does not affect more towards the crystallite size results almost same percentage of degradation. So, crystallite size is an important factor for degradation of 4-nitrophenol.

The activation temperature of TiO₂ influences the catalyst activity because it affects the physical properties of the crystal such as porosity, surface

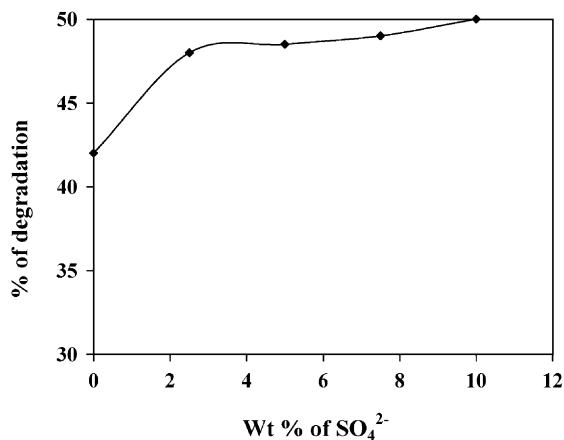


Fig. 9. Effect of wt.% of anions on the percentage of degradation.

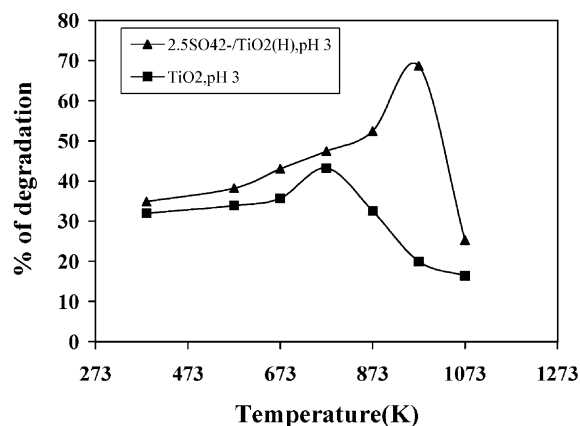


Fig. 10. Effect of activation temperature on the percentage of degradation.

area, and crystal structure as well as crystal size. Fig. 10 represents the effect of activation temperature of unmodified and sulphate-modified TiO₂ on the photocatalytic degradation of 4-nitrophenol. It is observed that the percentage of degradation gradually increases with increase in activation temperature up to 773 K and thereafter decreases for unmodified TiO₂. But the percentage of degradation increases with increase in activation temperature up to 973 K and thereafter decreases for sulphate-modified TiO₂. The percentage of degradation of 4-nitrophenol in case of sulphate-modified TiO₂ is higher than that of unmodified TiO₂ at all activation temperatures. The percentage of degradation is highest at 773 K activation for TiO₂ sample whereas 973 K for sulphated TiO₂ samples. This is due to the presence of mixture of anatase and rutile phases of TiO₂. The decrease in photocatalytic activity at higher activation temperature is perhaps due to loss of porous structure of nanoparticles, formation of denser particles due to sintering as well as transformation into rutile from anatase phase.

The present results can be directly compared with the data published earlier [5,6,11]. While optimising the reaction conditions, we found that 0.05 g/l of 4-nitrophenol can be completely degraded by using 0.6 g/l of sulphate-modified TiO₂ catalyst in 3 h under solar radiation. These results found better than those reported earlier with respect to the concentration of nitrophenol, amount of catalyst and time using UV radiation.

5. Conclusions

1. Modification of the hydrated titania with anions like sulphate can alter the specific surface area, crystallinity and transforms the bulk oxides to nanomaterials.
2. Methods of preparation and activation temperatures greatly affect the textural properties.
3. Photocatalytic degradation of 4-nitrophenol depends on surface area, phase and crystallite size of titania.
4. Complete decomposition of 4-nitrophenol (0.05 g/l) takes place using 0.6 g/l sulphated TiO₂ in 3 h.
5. Sulphated TiO₂ can be effectively used for degradation of 4-nitrophenol under solar radiation.

Acknowledgements

The authors are thankful to Dr. V.N. Misra, Director, Regional Research Laboratory (CSIR), Bhubaneswar, for giving permission to publish this paper. One of the authors, S.K.S. is obliged to CSIR, New Delhi, for a senior research fellowship.

References

- [1] M.S. Dieckmann, K.A. Gray, *Water Res.* 30 (1996) 1169.
- [2] N. Takahashi, T. Nakai, Y. Satoh, Y. Katoh, *Water Res.* 28 (1994) 1563.
- [3] F.J. Beltran, V. Gomez-Serrano, A. Duran, *Water Res.* 26 (1992) 9.
- [4] A. Pintar, J. Levec, *Chem. Eng. Sci.* 49 (1994) 4391.
- [5] V. Augugliaro, L. Palmisano, M. Schiavello, A. Sclafani, L. Marchese, G. Martra, F. Miano, *Appl. Catal. A: Gen.* 69 (1991) 323.
- [6] D. Chen, A.K. Ray, *Appl. Catal. B: Environ.* 23 (1999) 143.
- [7] R. Andreozzi, V. Caprio, A. Insola, G. Longo, V. Tufano, *J. Chem. Technol. Biotechnol.* 75 (2000) 131.
- [8] N. San, A. Hatipo Lu, G. Kocturk, Z. Cnar, *J. Chem. Technol. Biotechnol.* 146 (3) (2002) 189.
- [9] C.S. Turchi, D.F. Ollis, *J. Catal.* 122 (1990) 178.
- [10] G. Riegel, J.R. Bolton, *J. Phys. Chem.* 99 (1995) 4215.
- [11] A. Makowski, Z. Dziewiecki, W. Wardas, in: *Proceedings of the Presentation at the 17th Meeting of the North American Catalysis Society*, Toronto, 3–8 June 2001.
- [12] J. Kiwi, C. Pulgarin, P. Peringer, *Appl. Catal. B: Environ.* 3 (1994) 335.
- [13] N. Xu, Z. Shi, Y. Fan, J. Dang, J. Shi, M.Z.C. Hu, *Eng. Chem. Res.* 33 (2) (1999) 373.
- [14] A. Soni, R. Ameta, B. Sharma, S.C. Ameta, *J. Ind. Pollut. Control* 15 (1) (1999) 117.

- [15] Q. Zhao, J. Yu, X. Zhao, S. Mu, Taoci Xuebao 20 (3) (1999) 177.
- [16] Q. Dai, Z. Zhang, N. He, P. Li, C. Yuan, Mater. Sci. Eng. C8–C9 (1999) 417.
- [17] J. Grzechulska, M. Hamerski, A.W. Morawski, Water Res. 34 (5) (2000) 1638.
- [18] K.M. Parida, M. Acharya, S.K. Samantaray, T. Mishra, J. Colloid Interface Sci. 217 (1999) 388.
- [19] S.K. Samantaray, T. Mishra, K.M. Parida, J. Mol. Catal. A: Chem. 156 (2000) 267.
- [20] S.K. Samantaray, K.M. Parida, J. Mol. Catal. A: Chem. 176 (2001) 151.
- [21] W. Su, Y. Chen, X. Fu, K. Wei, Cuihua Xuebao 22 (2) (2001) 175.
- [22] J.-J. Du, A.-W. Xu, Y. Jing, Zhong-Shan Daxue Xuebao, Ziran Kexueban 40 (3) (2001) 48.
- [23] M. Sokmen, A. Ozkan, J. Photochem. Photobiol. 147 (1) (2002) 77.
- [24] P.H. Eglı, Growth and Perfection of Crystals, Wiley, New York, 1958, p. 408.
- [25] A.C. Walker, J. Franklin Inst. 250 (1950) 481.
- [26] K. Kandori, S. Uchida, S. Kataoka, T. Ishikawa, J. Mater. Sci. 27 (1992) 719.
- [27] D.G. Barton, S.L. Soled, G.D. Meitzner, G.A. Fuentes, E. Iglesia, J. Catal. 181 (1999) 57.
- [28] L.J. Almeny, M.A. Larrubia, M.C. Jimenez, F. Delgado, J.M. Blasco, React. Kinet. Catal. Lett. 60 (1) (1997) 41.
- [29] K. Nakamoto, Infrared and Raman Spectra of Inorganic and Coordination Compounds, 4th ed., Wiley, New York, 1986.
- [30] A.K. Dalai, R. Sethuraman, S.P.R. Katikanani, R.O. Idem, Ind. Eng. Chem. Res. 37 (1998) 3869.
- [31] B.H. Davis, R.A. Keogh, R. Srinivasan, Catal. Today 20 (1994) 219.
- [32] T. Lopez, P. Bosch, F. Tzompantzi, R. Gomez, J. Navarrete, E. Lopez-Salinas, M.E. Llanos, Appl. Catal. 197 (2000) 107.
- [33] R. Dillert, I. Fornefett, U. Siebers, D. Bahnemann, J. Photochem. Photobiol. A 94 (1996) 231.
- [34] H. Chen, E. Ruckenstein, J. Colloid Interface Sci. 148 (2) (1992) 382.
- [35] S.-J. Tsai, S. Cheng, Catal. Today 33 (1997) 227.
- [36] Q. Zhang, L. Gao, J. Guo, Appl. Catal. B 26 (2000) 207.
- [37] R.R. Basca, J. Kiwi, Appl. Catal. B 16 (1998) 19.
- [38] A.P. Rivera, K. Tanoka, T. Hisanaga, Appl. Catal. B: Environ. 3 (1993) 37.
- [39] A. Hagfeldt, M. Gratzel, Chem. Rev. 95 (1995) 49.